

On the Predictability of Underwater Acoustic Communications Performance: the KAM11 Data Set as a Case Study

Beatrice Tomasi^{*}, James Preisig[‡], Michele Zorzi^{*}

^{*}DEI, University of Padova — Via G. Gradenigo, 6/B, Padova, Italy

[‡]AOPE, Woods Hole Oceanographic Institution — 266 Woods Hole Rd., Woods Hole, MA, USA

{tomasibe,zorzi}@dei.unipd.it jpreisig@whoi.edu

ABSTRACT

In this paper, we analyze the predictability of the communications performance of an adaptive modulation system for underwater acoustic communications. As a case study, we consider the KAM11 data set, which has been collected off the coast of Kauai Island during July 2011. We measure the signal to noise ratio at the output of the equalizer and we observe slow fluctuations over time intervals of up to six minutes. Based on an analytical model and using the estimated time correlation coefficient of subsequent values of the signal to noise ratio (SNR), we compute the communications performance as a function of the feedback delay for an adaptive modulation system, and we evaluate its predictability. We show that it is possible to know in advance the trend of the performance over intervals of three to four minutes.

Categories and Subject Descriptors

C.2.0 [Communication/Networking and Information Technology]: General—*Data communications*; I.6.6 [Simulation and Modeling]: Simulation Output Analysis

General Terms

Measurement, Performance

Keywords

Underwater acoustic communications, predictability, simulation

1. INTRODUCTION

In this paper, we study the predictability of the communications performance of an adaptive modulation scheme in the underwater acoustic scenario. We analyze the KAM11 data set, collected during July 2011 off the coast of Kauai Island, in order to evaluate time fluctuations. Specifically, we estimate the time series of the SNR computed at the output of the equalizer and averaged over a packet, which indicates the average communication quality seen by the upper layers. These time series last six minutes, and are evaluated

over periods two hours apart. Finally we show the predictability, by using the estimated time fluctuations to set the parameters of the analytical model presented in [1], and we evaluate outage probability and throughput as functions of the lag between the feedback and the current Channel State Information (CSI).

The rationale behind this work is that by assessing the predictability of the "quality" of the communications channel and the resulting performance of underwater communications systems, we can determine the classes of feedback and adaptive communications techniques that are most suitable for a given underwater environment. The time scales of interest (several seconds to a few minutes) are very relevant to the performance of adaptive communications schemes and network protocols requiring control signaling.

Assessing the most appropriate techniques for providing and exploiting feedback is particularly important for the many half-duplex underwater acoustic communications systems such as those in [2] and [3]. In such systems, the use of feedback both reduces the capacity of the link and increases energy consumption. Nevertheless feedback (or control messages) is necessary to many communication techniques, such as Adaptive Modulation and Coding (AMC), power control, Automatic Repeat reQuest (ARQ), and to networking protocols. Therefore, unlike for the wireless terrestrial counterpart, not affected by the same restrictive constraints, it is important to assess the possibility of reducing the amount of feedback, without losing the advantages of more complex techniques.

In contrast to the study in [4], we focus on the predictability of the communications performance (output SNR), rather than of the channel impulse response. Measures of communications performance such as output SNR are more practical to send over an acoustic feedback channel and are more important when determining the next transmission parameters in an AMC context. In addition, we focus on performance averaged over the length of transmission packets because techniques like AMC are driven by conditions that change over inter-packet intervals. In [5], the authors provide a study on the predictability of the SNR computed on the received signal, which will be called input SNR later on, for the closed loop power control technique. As we will show in the following, for single carrier wide-band modulation schemes, such as that considered in [5], closed loop power control may not be as effective as it is commonly thought. Moreover, our work differs from the work in [5], in the considered environment and in the observed metric: in fact, even if assessing the predictability of the input SNR or of the output SNR is qualitatively equivalent, quantitatively it is not. The authors of [6] performed the first study taking into account outdated CSI, but they did not study the possibility of decreasing the feedback rate. Moreover, none of the studies on underwater network protocols, such as [7], [8], [9], [10] and [11] deals

Permission to make digital or hard copies of all or part of this work for personal or classroom use is granted without fee provided that copies are not made or distributed for profit or commercial advantage and that copies bear this notice and the full citation on the first page. To copy otherwise, to republish, to post on servers or to redistribute to lists, requires prior specific permission and/or a fee.

WUWNet'11, Dec. 1 - 2, 2011, Seattle, Washington, USA
Copyright 2011 ACM 978-1-4503-1151-9 ...\$10.00.

with or takes advantage of time correlated channel conditions. Indeed, differently from the terrestrial radio communications, where the transmission rates and propagation delays are negligible with respect to the time-varying channel conditions in a stationary scenario, the underwater case is more heavily affected by environmental changes of the order of several seconds, so that these effects should be considered when optimizing or designing new networking protocols. This approach appears, for the first time, in [12], where the authors observe via simulation that changes in the sound speed profile conditions affect the performance of MAC and routing protocols. Nevertheless, they do not study the predictability of such varying conditions, but they rather suggest to use more control messages.

AMC techniques aim at maximizing the spectral efficiency, by taking advantage of the known CSI. Such spectral efficiency is upper bounded by the system capacity. As far as the authors' knowledge, the problem of determining the capacity of a frequency selective system with feedback delay and outdated CSI remains an open problem, even though it has been intensively studied (for example in [13], [14] and [15]) from an information theoretic point of view.

Therefore, for the reasons discussed so far, in this paper we study the predictability of the communications performance over a link, by focusing on the AM context, and we provide some evidence on the order of time-fluctuations over intervals six minutes long, which is of interest for a large number of networking protocols and applications, by using experimental data. The results presented here are computed over a subset of the KAM11 data, described below. The examined subset refers to 62 percent of the total collected epochs from Julian date 185 to 190, and the observations here hold for 53 percent of that data subset. The remaining 47 percent of the processed data presents bad channel conditions, which limited the equalizer performance, thus leading to inaccurate results. In addition, as a next step, the environmental data will be processed, so that an evaluation of what factors are contributing to the poor equalizer performance will become clearer. Given that our main scope is the use of feedback to adapt transmission parameters, we focus only on the part of the data characterized by good channel conditions. A more complete description of the collected data set, that was designed for the objectives described previously, can be found in Section 2, whereas the system model is presented in Section 3 and the results and conclusions are in Section 4 and 5, respectively.

2. EXPERIMENTAL DATA SET

In this section, we describe the considered experimental scenario and we show a first evaluation of the measured channel characteristics.

2.1 Scenario

The KAM11 data set has been collected in 2011 during Julian dates from 171 to 191, off the coast of Kauai Island. In this paper, we analyze the subset of data transmitted and recorded by the WHOI Autonomous System, from Julian date 185 to 190, during which our specific signal was transmitted. The scenario was stationary: the source and the receiver were 3 km apart and positioned at 45 m below the ocean surface. The receiver used signals received at a 24 element vertical and linear hydrophone array with 5 cm spacing between hydrophones. The equalizer used to generate the results shown here utilized signals from 4 of the hydrophones spaced by 15 cm. The central frequency and bandwidth of the omni-directional source were 13 kHz and 8 kHz, respectively.

Conductivity, temperature and depth (CTD) data have been collected during the experiments, and we can observe in Figure 1 the

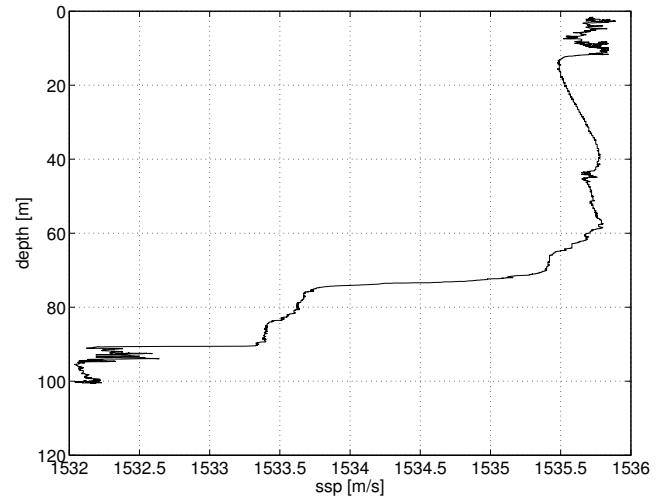


Figure 1: Sound Speed Profile collected on Julian date 176 off the coast of Kauai Island.

Sound Speed Profile (SSP) estimated from one such CTD measurement. We can assume that the whole area is characterized by the same SSP, even though the thermocline, which in Figure 1 is around 70 m below the surface, might slightly change due to the propagation of internal waves. The SSP is down-refractive from the surface to 15 m, from where it becomes up-refractive up to 60 m and it ends as down-refractive again. This particular combination of up and down-refractive parts in the water column gives rise to different propagation paths, which are very sensitive even to a slight change of the SSP in time. From the data collected by a thermistor chain, it is possible to follow those time fluctuations and correlate them with the variations observed in the channel impulse responses. This data analysis and a ray-tracer simulation are part of future investigations and will help in understanding the effects of this type of SSP on the communication performance.

The source transmits six sound files every two hours. Each file consists of an initial period of silence, a train of 31 packets, separated in time by 280 ms in order to avoid interference between contiguous packets, and a couple of longer packets which will not be analyzed in this study. Overall, the file lasts one minute (including also silence), and in this study we will focus on the 31 data packets, each containing 6500 modulation symbols, transmitted at 6250 symb/s. This data set allows us to study the time variability of the communications performance in different environmental conditions. In particular, we can analyze how much environmental conditions such as surface roughness, internal waves, temperature gradients and wind speed, affect the propagation and the received signal quality.

2.2 Channel impulse response

During the experiments, the BPSK and QPSK modulated data were preceded by a sequence of Linear Frequency Modulated (LFM) pulses, transmitted in order to have a first raw estimate of the channel impulse response. In this section, we show the results relative to the LFM pulses, by choosing a couple of representative samples of the extensive subset analyzed. We will focus in particular on date 187 at different hours.

Figures 2 and 3 represent the pseudocolor of the amplitude of the channel impulse responses obtained by processing LFM pulses. The y-axis is the observation time in minutes, and the x-axis is

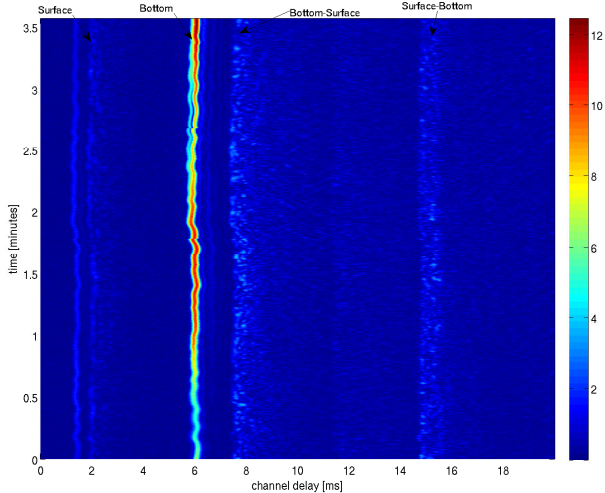


Figure 2: Pseudocolor of the time series of the estimated amplitude of the channel impulse response. Date 187 at 4 am, when the receiver has good performance.

the delay of the channel arrivals in milliseconds. As mentioned in the Introduction, the receiver works in the acceptable regime of SNR (from a few dB up) only on a part of the whole processed data set. Here we show the conditions of the channel when the receiver works and when it does not, and we highlight the channel characteristics that make the difference.

For example, in Figure 2, we observe a strong consistent arrival, which can be used for synchronization, and even if its amplitude changes over time, it is the stablest and the strongest of all arrivals. On the other hand, the channel conditions represented in Figure 3 are more rapidly varying, so that it is harder to identify a stable arrival throughout the time series. These conditions give rise to synchronization problems, thus resulting in very poor decoding performance.

From the measured channel impulse response, we can estimate some channel parameters such as delay and Doppler spread, in order to define the context of our case study. For now we do not evaluate quantitatively such channel parameters, but by observing Figures 2 and 3 we can assess that the channel can be doubly selective, both in time and in frequency, and it has time-varying degrees of selectivity. For example the channel depicted in Figure 2 can be defined as slow time-varying and frequency selective, whereas the channel in Figure 3 is fast time-varying and frequency selective. From now on, we will focus on those recorded signals that were affected by channel impulse responses similar to those shown in Figure 2.

3. SYSTEM MODEL AND PERFORMANCE

In this section, we describe the communication system under analysis. For the moment, we consider only an adaptive modulation (AM) scheme with no channel coding, since our focus is more on understanding the effects of correlated time fluctuations on this technique, rather than designing a new adaptive scheme. In any event, the extension to the AMC case would be straightforward and would not give much different results. According to the AM technique, the transmitter can change the constellation size based on the CSI fed back by the receiver. This mechanism improves the spectral efficiency of the communication system, by taking advantage of the knowledge of changing channel conditions. On the

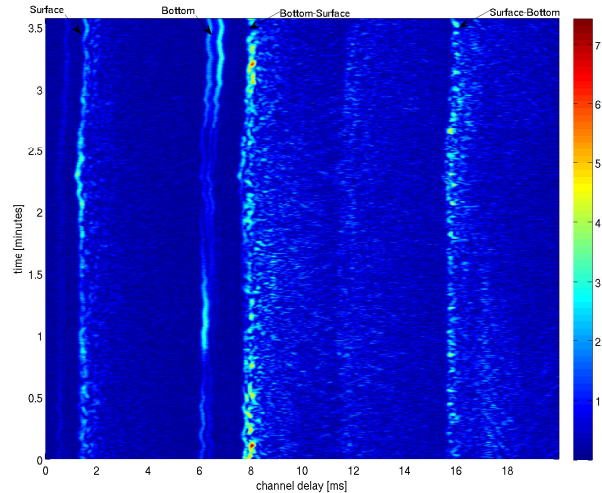


Figure 3: Pseudocolor of the time series of the estimated amplitude of the channel impulse response. Date 187 at 8 am, when the receiver cannot decode.

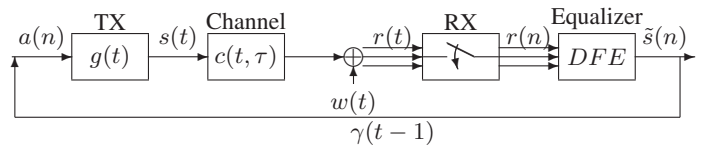


Figure 4: System model. The SNR, $\gamma(t-1)$, is estimated after the equalizer and is fed back to the receiver. The symbol $r(t)$ represents the vector of the received symbols at different receiver elements.

other hand, CSI may reach the transmitter after some propagation and decoding delay, thus becoming outdated.

3.1 System model

Figure 4 represents the considered Single Input Multiple Output (SIMO) system model. Modulation symbols, $a(n)$, are transmitted over the channel, $c(t, \tau)$, which introduces distortion, and they are received with additive noise $w(t)$ at the receiver side at different depths. At the receiver side, after synchronization, the received signals are re-sampled, combined, and processed by a Decision Feedback Equalizer (DFE). Then, the output symbol SNR, γ , is estimated from the software decision at the output of the equalizer, $\tilde{s}(n)$, and is then fed back. The transmitter, based on a predefined Quality of Service (QoS) requirement, decides for the largest constellation size which assures such QoS. In our case, we consider constant modulus constellations, such as M Phase Shift Keying (M -PSK), with $M \in \{2, 4, 8\}$, and we choose as QoS the maximum Bit Error Rate (BER), here 10^{-3} , for the transmitted bit stream. We compute the BER as a function of the average symbol SNR γ , by assuming that the received $\tilde{s}(n)$, inside a packet, is affected by only AWGN, so that we can use the following equations [16]:

$$P_b(M; \gamma) = \begin{cases} Q(\sqrt{2\gamma}), & M = 2 \\ Q(\sqrt{\gamma}), & M = 4 \\ \frac{2}{3} Q(\sqrt{2\gamma} \sin(\pi/8)), & M = 8. \end{cases} \quad (1)$$

Given a maximum BER, we compute the set of threshold SNRs, which are associated to each constellation size M .

We express the software decision as

$$\tilde{s}(n) = \tilde{c}(0)a(n) + \tilde{w}(n), \quad (2)$$

where $\tilde{c}(0)$ is the residual channel coefficient after equalization and \tilde{w} is the residual additive noise, which includes noise and residual ISI. We assume that $\tilde{c}(0)$ is constant over a packet but varies slowly across different packets (we saw in Section 2 that this assumption holds).

From Equation (2) we define the average output SNR as

$$\gamma = \frac{|\tilde{c}(0)|^2 E_s}{\sigma^2}, \quad (3)$$

where E_s is the energy of the modulation symbol and σ^2 is the variance of the residual noise \tilde{w} . Given that we consider constant modulus constellations, E_s is one for every symbol. We estimate the residual channel coefficient for each packet as the average of the software decision divided by the corresponding transmitted signal, so that it does not depend on the specific transmitted symbol. Then, we can write the residual coefficient as:

$$\tilde{c}(0) = \mathbb{E} \left[\frac{\tilde{s}(n)}{a(n)} \right]. \quad (4)$$

Given that w is a zero-mean process, this estimator is unbiased. Finally, we estimate σ^2 as:

$$\sigma^2 = \mathbb{E} [|\tilde{s}(n) - \tilde{c}(0)a(n)|^2]. \quad (5)$$

We can interpret $\tilde{c}(0)$ as the average residual channel coefficient over a packet, and σ^2 as the corresponding mean square error.

In the adaptive modulation context, we are interested in evaluating the changes of channel conditions over consecutive packets, in order to assess whether or not the fed back information is sufficient, if not outdated, to get the expected performance improvement. Specifically, we focus on the fluctuations of the output SNR in Equation (3), which is proportional to the squared amplitude of the average residual channel coefficient and is a measure of the received signal quality seen by the upper layers in the protocol stack. Given that we are observing an average output SNR, and given that the transmitter and receiver are stationary, we do not expect rapid fluctuations, but given that both the feedback delay and the processing time at the receiver are of the order of seconds, we do expect changes in the channel state over this time scale, as observed in Section 2.2.

We characterize the amplitude of the residual channel coefficient as a Nakagami random variable fully described by its second order statistics and with the following probability density function:

$$f(x) = \frac{2m^m}{\Gamma(m)\bar{c}^m} x^{2m-1} \exp\left(-\frac{m}{\bar{c}}x^2\right), \quad (6)$$

where $x = |\tilde{c}(0)|$. By substituting the variable $x^2/\sigma^2 = \gamma$, we get the probability density function for the output SNR, γ :

$$f(\gamma) = \frac{m^m}{\Gamma(m)\bar{\gamma}^m} \gamma^{m-1} \exp\left(-\frac{m}{\bar{c}}\gamma\right). \quad (7)$$

We choose this model because, thanks to the parameter m , it makes it possible to consider different fading shapes (from Rayleigh to Rice), and given that the distribution is completely defined by its second order statistics, it can be easily estimated from the time series. We then assume that two consecutive SNR samples, separated by a time interval τ , γ and γ_τ , are Nakagami correlated random variables, described by the following conditioned probability den-

sity function:

$$f(\gamma_\tau|\gamma) = \frac{m}{(1-\rho(\tau))\bar{\gamma}} \left(\frac{\gamma_\tau}{\rho(\tau)\gamma}\right)^{(m-1)/2} \times I_{m-1} \left(\frac{2m\sqrt{\rho(\tau)\gamma\gamma_\tau}}{(1-\rho(\tau))\bar{\gamma}} \right) \exp\left(\frac{m(\rho(\tau)\gamma + \gamma_\tau)}{(1-\rho(\tau))\bar{\gamma}}\right), \quad (8)$$

where $\rho(\tau)$ is the correlation coefficient between γ_τ and γ , and $I_{m-1}(\cdot)$ is the modified Bessel function of the first kind and of order $m-1$. This correlated model has been proposed initially in [1].

3.2 Communications Performance: outage probability and throughput

Here, we present a derivation of the communications performance for the AM system. In particular, we focus on outage probability and average throughput as functions of feedback delay. The outage probability is a measure of how likely the event of not satisfying the QoS is, when using the constellation size associated to the fed back SNR value, γ . The average throughput is the mean amount of information per unit of time that is correctly received, and represents the tradeoff between high spectral efficiency and unreliable transmission.

We compute the outage probability, given a fed back γ , as the probability that γ_τ is less than the SNR threshold $T(\gamma)$, i.e., the inferior extreme of the SNR region associated to γ , which in symbol is

$$P(\gamma_\tau|\gamma) = \int_0^{T(\gamma)} f(\gamma_\tau|\gamma) d\gamma_\tau. \quad (9)$$

This conditional probability can be averaged over all the possible values for γ , including the case in which γ is less than the minimum average symbol SNR assuring the QoS, which will be indicated as T_1 . This outage probability is

$$P(\tau) = \int_{T_1}^{+\infty} f(\gamma) \int_0^{T(\gamma)} f(\gamma_\tau|\gamma) d\gamma_\tau d\gamma + \int_0^{T(1)} f(\gamma) d\gamma. \quad (10)$$

We compute the throughput as the average amount of information per second per Hertz, that is transmitted based on the fed back SNR γ and is correctly received. Given γ , the transmitter chooses the constellation size $M(\gamma)$, for which the number of bits per symbol is $b(\gamma) = \log_2(M(\gamma))$. By assuming the usage of an interleaver over the bit stream, we can compute the average throughput, given γ , as

$$\Theta(\tau|\gamma) = \int_{T(\gamma)}^{+\infty} b(\gamma)(1 - BER(\gamma_\tau))f(\gamma_\tau|\gamma) d\gamma_\tau, \quad (11)$$

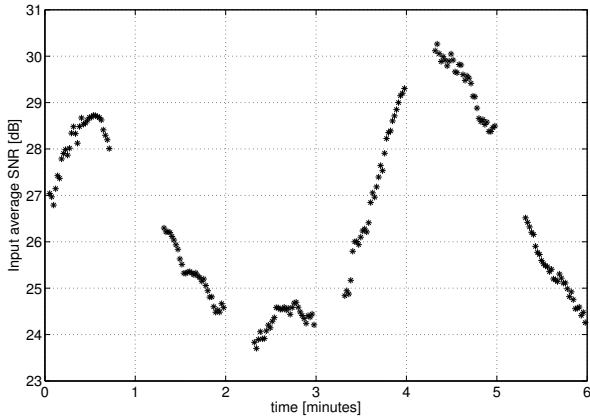
which, by considering all possible values for γ , becomes:

$$\Theta(\tau) = \int_{T_1}^{+\infty} f(\gamma)b(\gamma) \int_{T(\gamma)}^{+\infty} (1 - BER(\gamma_\tau))f(\gamma_\tau|\gamma) d\gamma_\tau d\gamma. \quad (12)$$

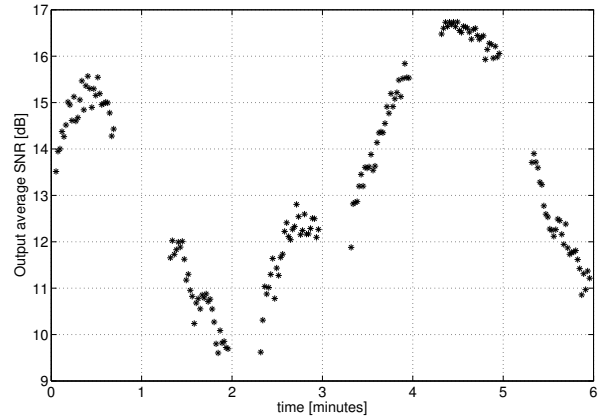
It is worth noticing that when γ_τ is less than the inferior extreme of the region associated to γ , i.e., if $\gamma_\tau < T(\gamma)$, the throughput is zero, because the QoS is not met.

4. RESULTS

In this section, we present the evaluation of the previous analysis based on the KAM11 data set. We first quantify the time changes of the average output SNR, and then we assess the predictability of the AM system performance.

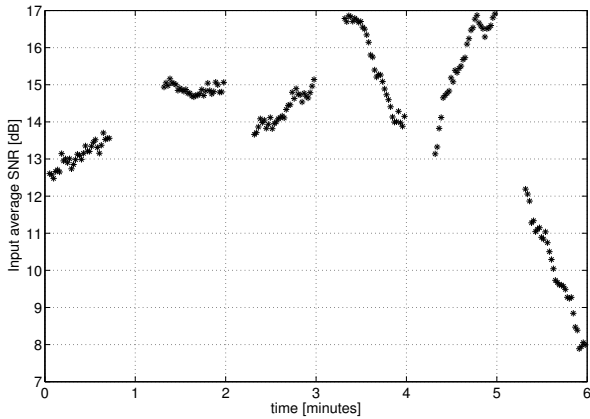


(a) Average input SNR at Julian date 187, at 4 am.

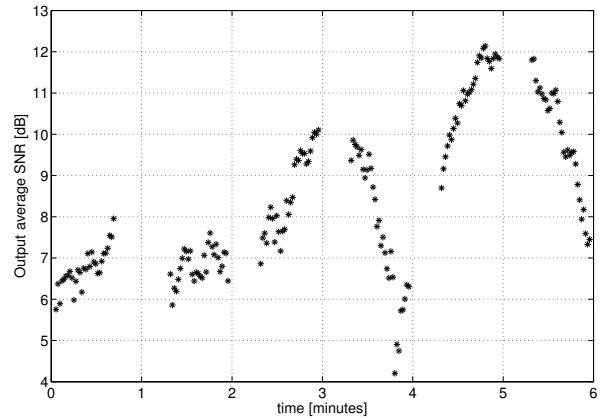


(b) Average output SNR at Julian date 187, at 4 am.

Figure 5: Julian date 187, at 4 am.



(a) Average input SNR at Julian date 188, at 00 am.



(b) Average output SNR at Julian date 188, at 00 am.

Figure 6: Julian date 188, at 00 am.

4.1 Time series of the average output symbol SNR

We show here the time series of the observed SNRs over an interval of six minutes at 4 am on Julian date 187 and at 00 am on date 188. The length of the observation interval allows us to measure the fluctuations of the SNR due to both rapid and slow environmental changes such as surface conditions and internal waves.

In Figures 5(b) and 6(b) we plot the estimated output symbol SNR, averaged over a packet and computed as in Equation (3), at times 4 am and 00 am, respectively. The used parameters for the DFE are: a feed-forward filter length of 1 ms, a feedback filter length of 10 ms, and we are combining the received signals at channels 1, 4, 7 and 10, which respectively are 45.55 m, 45.4 m, 45.25 m and 45.1 m below the surface.

Over the observation interval, the SNR varies between 9 and 17 dB at 4 am, and between 4 and 12 dB at 00 am, thus confirming the suitability of adaptive schemes that can take advantage of such changes. Nevertheless, an outdated channel state information can decrease the packet reliability, thus losing the advantage of adaptive modulation schemes. We observe a quite smooth and almost periodic fluctuation, in both Figures 5(b) and 6(b). In fact, we can see an increased SNR at minutes one and five in Figure 5(b), and

at minutes three and five in Figure 6(b). This behavior is suitable for predicting the communication system performance over subsequent packets.

Figures 5(a) and 6(a) show the average packet input SNR, which is computed as the ratio between the average energy of the received packet and the in band noise power measured before the train of packets. We observe the same fluctuations that we notice for the output SNR, even though the input SNR varies between 24 and 30 dB in Figure 5(a) and between 7 and 17 dB in Figure 6(a). The correlation between the input and output SNRs is more evident in Figure 5 than in Figure 6, because for that epoch the strongest arrival was not always the most stable. The gap between the input and output SNR represents the loss due to ISI and shows how strong the most stable arrival is relative to the other arrivals. We measure and show the input SNR, in order to test and prove that the fluctuations observed for the output SNR were caused by the environment and not by the post-processing on the data. Given that we observe the same almost periodical behavior for the average input and output SNRs, we can conclude that those fluctuations are environment-driven.

We can also observe that the decrease or increase rate of the input and output SNR are slightly different, thus suggesting that the

relative strength of the most stable arrival to the multipaths arrivals is not constant over time, but rather depends on the rapidly varying not-consistent arrivals, causing ISI. Comparing Figures 5 and 6, we can also notice that higher input SNRs, such as those in Figure 5(a), do not always correspond to an equivalent improvement of the output SNRs. For example, we observe a gap between the input SNRs, at dates 187 and 188 around the sixth minute, of about 16 dB, while the corresponding gap between the output SNRs is only about 4 dB. This means that, for the system under consideration (wide-band, single carrier), if we increase the transmission power, we do not always get correspondingly better communications performance. This is why, in a frequency selective scenario, power control and adaptive modulation techniques do not have the same performance. In this case, power control would not improve the system performance as much as an updated adaptive modulation scheme would.

We next evaluate the system performance when these time fluctuations are taken into account.

4.2 Predictability of the communications performance

A process is said to be predictable in time, when it is possible to know its value some time τ ahead. The process that we want to be able to predict is the average AM system performance in terms of throughput and outage probability. The analytical model, proposed in Section 3, depends only on the second order statistics of two correlated Nakagami variables, i.e., we only need to study the correlation coefficient between γ and γ_τ . Moreover, linear predictors are based on the second order statistics of the process that they track, so that from this study we can also conclude whether or not they can be a valuable class of predictors, and if so over which time scales. In the following we assume that the output SNR is a stationary random process, so that we can estimate the correlation coefficient. The stationarity of the SNR process was verified in [17], for the non-coherent case.

We indicate the correlation coefficient between two consecutive SNRs, γ and γ_τ , separated in time by τ , as $\rho(\tau)$ and compute it as:

$$\rho(\tau) = \frac{Cov(\gamma, \gamma_\tau)}{\sqrt{Cov(\gamma)C(\gamma_\tau)}}, \quad (13)$$

where $Cov(\cdot)$ is the covariance function defined as $Cov(x, y) = E[(x - m_x)(y - m_y)]$ and, if the function has only one variable, it is equivalent to computing the variance of the variable. Figure 7 shows the correlation coefficient $\rho(\tau)$ as a function of time within the six minute observation interval. Here we present $\rho(\tau)$ at three different hours: 2 am and 4 am on Julian date 187 and 00 am on 188. Given that for each minute we have the data for 31 packets, and given that each packet lasts 1 s, we interpolate the data in order to fill the gaps on the time series. For this reason we can observe a step-like behavior in Figure 7 between each minute and the next one. It is worth noticing that the shapes of the correlation functions at hours 2 and 4 am are quite alike, i.e., there is a second local maximum on the correlation function around the fourth minute, and then it decreases. This observation suggests that there are slowly changing environmental conditions which determine the shape of such correlation functions. The third curve, referring to date 188, is measured almost one day after the other two curves, and we can see how the shape of the correlation function has changed. In fact for this curve we note two other local maxima around the third minute and the fifth minute. The cause of such behavior has not been studied yet, but as a next step we will analyze the environmental data and propagation models, trying to explain these trends.

We now evaluate the average AM communications system per-

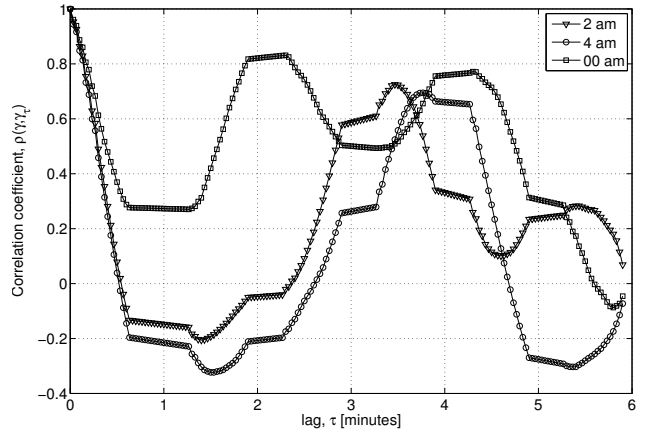


Figure 7: Correlation coefficient between two consecutive SNRs, τ minutes apart in time.

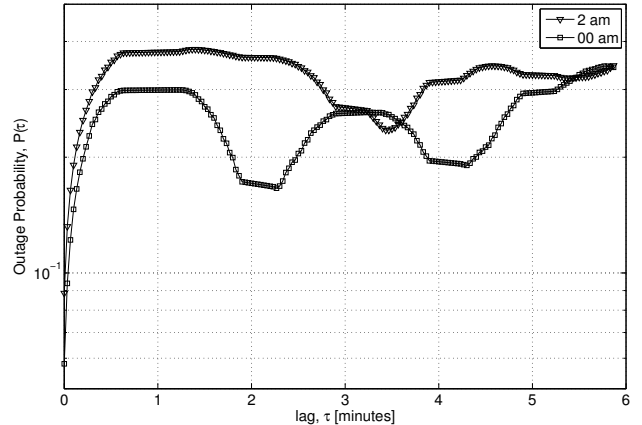


Figure 8: Outage probability as a function of τ .

formance, by applying Equations (11) and (12) and using the correlation coefficients $\rho(\tau)$ evaluated from the data. In particular, we estimate the parameter m for the Nakagami probability distribution, as $m = \frac{\bar{\gamma}^2}{E[(\gamma - \bar{\gamma})^2]}$, whereas we do not compute the average SNR $\bar{\gamma}$ from the data, but we assume the same one (10 dB) for all the considered hours, in order to get comparable results, and in order to highlight the effects on the performance of the time fluctuations.

Figures 8 and 9 show the system performance as functions of the feedback delay τ . Doubtless, a feedback delay of the order of minutes is not of great practical interest, but we aim at understanding over which time interval the process can be predictable, in order to prove that the feedback rate can be decreased. As expected, corresponding to the local maxima of the correlation function, we find local minima for the outage probability and local maxima for the throughput. This means that if we knew the system performance at the present time, we could expect similar performance in four minutes as shown by the curve representing hour 2 am, and in three and five minutes as shown by the curve representing time 00 am. We prove here that the time behavior of an adaptive system performance permits predictability, and we show how far ahead this holds.

These results give rise to several considerations on how to take

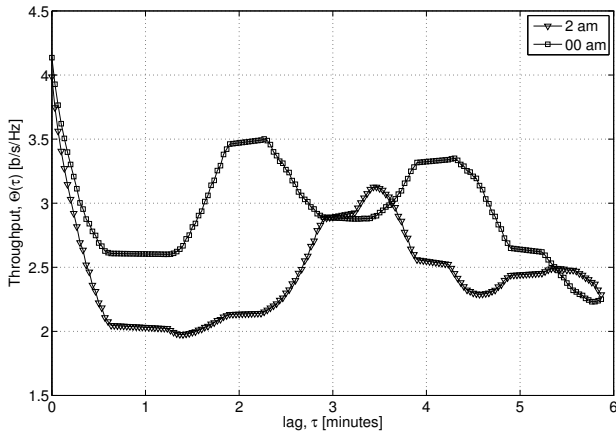


Figure 9: Throughput as a function of τ .

advantage of such predictability when designing communications and networking algorithms. For what concerns adaptive modulation schemes, we should be able to answer the following open questions: which feedback information about the channel state is most effective in enhancing the performance? Is the feedback rate adjustable without any performance loss? Which predictors are more suitable to indicate the next transmission parameters? For example, so far we assumed that the previous average output SNR γ provides sufficient information to choose the best next transmission parameters, but if we want to decrease the feedback rate, this may no longer be the case. Indeed, as shown in Figures 8 and 9, the information about the next time when a local maximum occurs in the correlation coefficient can be more useful to adjust accordingly the system parameters and it would not require the same amount of feedback, thus saving energy and channel occupancy.

Moreover, we can also say that knowing the time between two highly correlated instants can be very useful for networking protocols. For example, a routing protocol could take advantage of such information by updating the routing tables accordingly or a medium access control protocol could assign the best slot of time to different nodes according to different local fluctuations that they observe.

5. CONCLUSIONS AND FUTURE WORK

In this paper, we have studied the predictability of the communications performance for an underwater acoustic scenario, based on experimental data. The data have been collected during July 2011, off the coast of Kauai Island. We have analyzed the data set from a shallow water deployment and we have presented here the results on a few representative epochs. In particular, we have focused on the AM scheme, and we have evaluated its performance as a function of the feedback delay.

From the obtained results, we can define some guidelines for future studies. In fact, we will evaluate the performance of different predictors, and we will investigate which environmental conditions are causing such fluctuations. Moreover, we will think of new solutions for networking protocols, which exploit the high time correlation, measured during the analyzed data set.

Acknowledgment

The authors would like to thank all the people involved in the KAM11 experiment. Moreover we would like to thank Dr. Laura Toni, for her initial guide on the adaptive modulation study. This

work has been supported by ONR under Grants no. N00014-10-10422, N00014-05-10085 and N00014-07-10738.

6. REFERENCES

- [1] M. S. Alouini and A. J. Goldsmith, "Adaptive modulation over Nakagami fading channels," in *Springer J. on Wireless Personal Commun.*, vol. 13, no. 1–2, pp. 119–143, May, 2000.
- [2] "Teledyne benthos undersea systems," www.benthos.com.
- [3] L. Freitag, M. Grund, S. Singh, J. Partan, P. Koski, and K. Ball, "The WHOI Micro-Modem: An Acoustic Communications and Navigation System for Multiple Platforms," <http://www.whoi.edu>, 2005.
- [4] A. Radosevic, T. M. Duman, J. G. Proakis and M. Stojanovic, "Channel prediction for adaptive modulation in underwater acoustic communications," in *Proc. IEEE OCEANS*, Spain, Jun., 2011.
- [5] P. Qarabaqi and M. Stojanovic, "Adaptive power control for underwater acoustic communications," in *Proc. IEEE OCEANS*, Spain, Jun., 2011.
- [6] B. Tomasi, L. Toni, P. Casari, L. Rossi and M. Zorzi, "Performance study of variable-rate modulation for underwater communications based on experimental data," in *Proc. MTS/IEEE OCEANS*, Seattle, USA, Sep., 2010.
- [7] M. Molins and M. Stojanovic, "Slotted FAMA: a MAC Protocol for underwater networks," in *Proc. MTS/IEEE Oceans*, Singapore, Sep. 2006.
- [8] A. Syed, W. Ye, and J. Heidemann, "Comparison and Evaluation of the T-Lohi MAC for Underwater Acoustic Sensor Networks," in *IEEE J. Select. Areas Commun.*, vol. 26, pp. 1731–1743, Dec. 2008.
- [9] B. Peleato and M. Stojanovic, "Distance aware collision avoidance protocol for ad hoc underwater acoustic sensor networks," in *IEEE Commun. Lett.*, vol. 11, no. 12, pp. 1025–1027, Dec. 2007.
- [10] K. Kredo and P. Djukic and P. Mohapatra, "STUMP: exploiting position diversity in the staggered TDMA underwater MAC protocol," in *Proc. IEEE INFOCOM*, Rio de Janeiro, Brazil, Apr., 2009.
- [11] K. Kredo and P. Mohapatra, "Distributed scheduling and routing in underwater wireless networks," in *Proc. IEEE GLOBECOM*, Miami, USA, Dec., 2010.
- [12] S. Azad, P. Casari, C. Petrioli, R. Petrocchia, and M. Zorzi, "On the impact of the environment on MAC and routing in shallow water scenarios," in *Proc. IEEE OCEANS*, Spain, Jun., 2011.
- [13] H. Viswanathan, "Capacity of Markov channels with receiver CSI and delayed feedback," in *Proc. IEEE ISIT*, Aug., 1998.
- [14] A. J. Goldsmith and M. Medard, "Capacity of time-varying channels with causal channel side information," in *IEEE Trans. on Information Theory*, vol. 53, no. 3, pp. 881–899, Mar., 2007.
- [15] S. Tatikonda and S. Mitter, "The capacity of channels with feedback," in *IEEE Trans. on Information Theory*, vol. 55, no. 1, pp. 323–349, Jan., 2009.
- [16] A. J. Goldsmith, *Wireless Communications*, pp 162. Cambridge University Press, 2005.
- [17] B. Tomasi, J. Preisig, G. B. Deane and M. Zorzi, "A study on the wide-sense stationarity of the underwater acoustic channel for non-coherent communication systems," in *Proc. European Wireless*, Vienna, Apr., 2011.